P-58: Optimization of the Luminous Efficiency of Plasma Display Panels Using Numerical Modeling

Georgios Veronis, and Umran S. Inan
Space, Telecommunications, and Radioscience Laboratory, Stanford University, Stanford, California, 94305

Abstract
A two-dimensional model is used to study the effect of cell structure on the performance of PDPs. More specifically, the effect of the insertion of a floating conducting material between the dielectric layer and the MgO film on the performance of the device is investigated. The shape of the discharge power pulse is found to be significantly different in comparison with the corresponding pulse of the standard cell geometry. It is also found that this cell structure results in a more confined discharge.

1. Introduction
Plasma display panels (PDPs) are one of the leading candidates in the competition for large-size, high-brightness flat panel displays, suitable for high-definition television monitors.

PDP cells are small and provide limited access for diagnostic measurements. PDP parameters which can be measured experimentally are still insufficient to provide a quantitative understanding of the discharge dynamics. As a result, computer modeling is currently essential for understanding PDP physics and optimizing its operation [1,2]. The goal of this work is to use two-dimensional simulations to provide better understanding of the underlying physics that determine the efficiency of the cell structure. More specifically, we investigate the effect of the insertion of a floating conducting material between the dielectric layer and the MgO film on the performance of the device. Such an arrangement has recently been proposed as a way to substantially increase the luminous efficiency [3].

2. Model Description
The model utilized here is based on a self-consistent simulation of the microdischarges in the PDP cell. The space and time variation of the electric field within the cell is self-consistently determined by solving the fluid equations for ions (Ne^+,Xe^+) and electrons together with Poisson's equation, subject to the boundary conditions imposed by the electrode boundaries. The electrical model is coupled to a model of excited species kinetics ($Xe^*(^3P_1)$, $Xe^*(^3P_2)$, Xe^{**}, $Xe_2^*(O_u^+)$, $Xe_2^*(^3\Sigma_u^+)$, $Xe_2^*(^1\Sigma_u^+)$) and UV emission at 147 nm, 150 nm, and 173 nm. The electron-impact ionization and excitation frequencies as well as the electron drift velocity are calculated as a function of the reduced electric field *E/N* using the Boltzmann code ELENDIF [4]. A semi-implicit numerical technique is used for the solution of the system of equations [5]. The capacity matrix method [6] is used for the numerical treatment of the floating conducting electrodes inserted in the dielectric layer.

3. Results
3.1 Cell Geometry and Driving Waveform
The geometry of the PDP cell used in the simulations is shown in Figure 1a. The relative permittivity of the dielectrics is 10. The gas mixture filling the region between the dielectrics is a 4% Xe-Ne mixture at a pressure of 500 Torr. The secondary electron emission coefficients for Ne and Xe ions on MgO are taken to be 0.5 and 0.01 respectively. The width of the cell *L* is 1260 μm, the gas gap length *D* is 150 μm, and the thickness of the dielectric layers *d* is 30 μm. The width *w* of the X and Y electrodes is set to 300 μm.

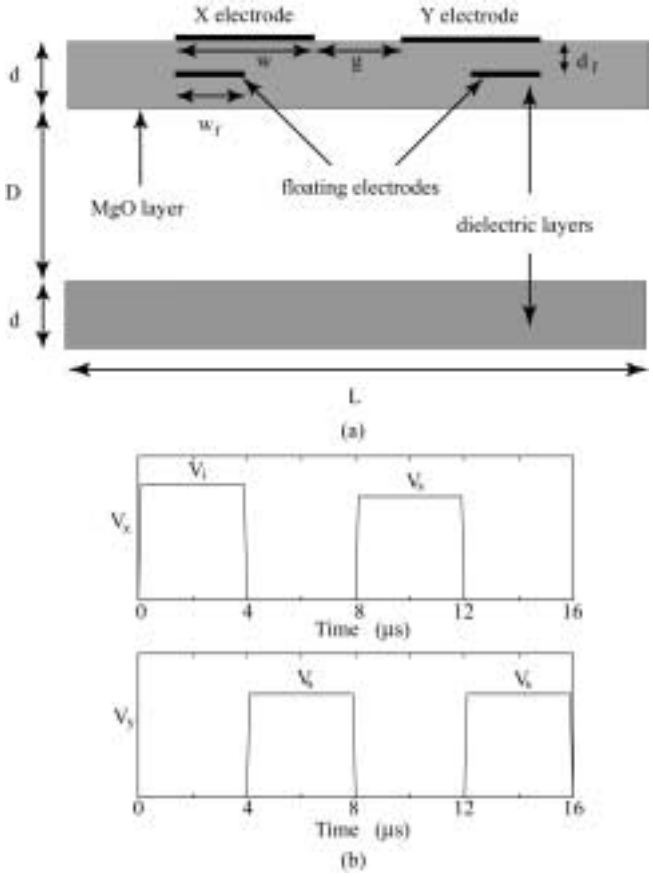

Figure 1. (a) Schematic of PDP cell. (b) Applied voltage waveforms.

In order to compare our results with the results reported in [3], we only apply sustain pulses between the X and Y electrodes, as is shown in Figure 1b. We do not include the address electrode in the simulation results reported here. The driving voltage waveform consists of a sequence of 4 μs pulses (Figure 1b). The rise and fall times of all pulses are 100 ns. A pulse of amplitude V_i is first applied on the X electrode to cause breakdown and form an initial charge distribution on the surface of the upper dielectric layer. This is followed by a sequence of alternating sustaining voltage pulses of amplitude V_s.

 ISSN/0001-0966X/01/3201-0770-$1.00+.00

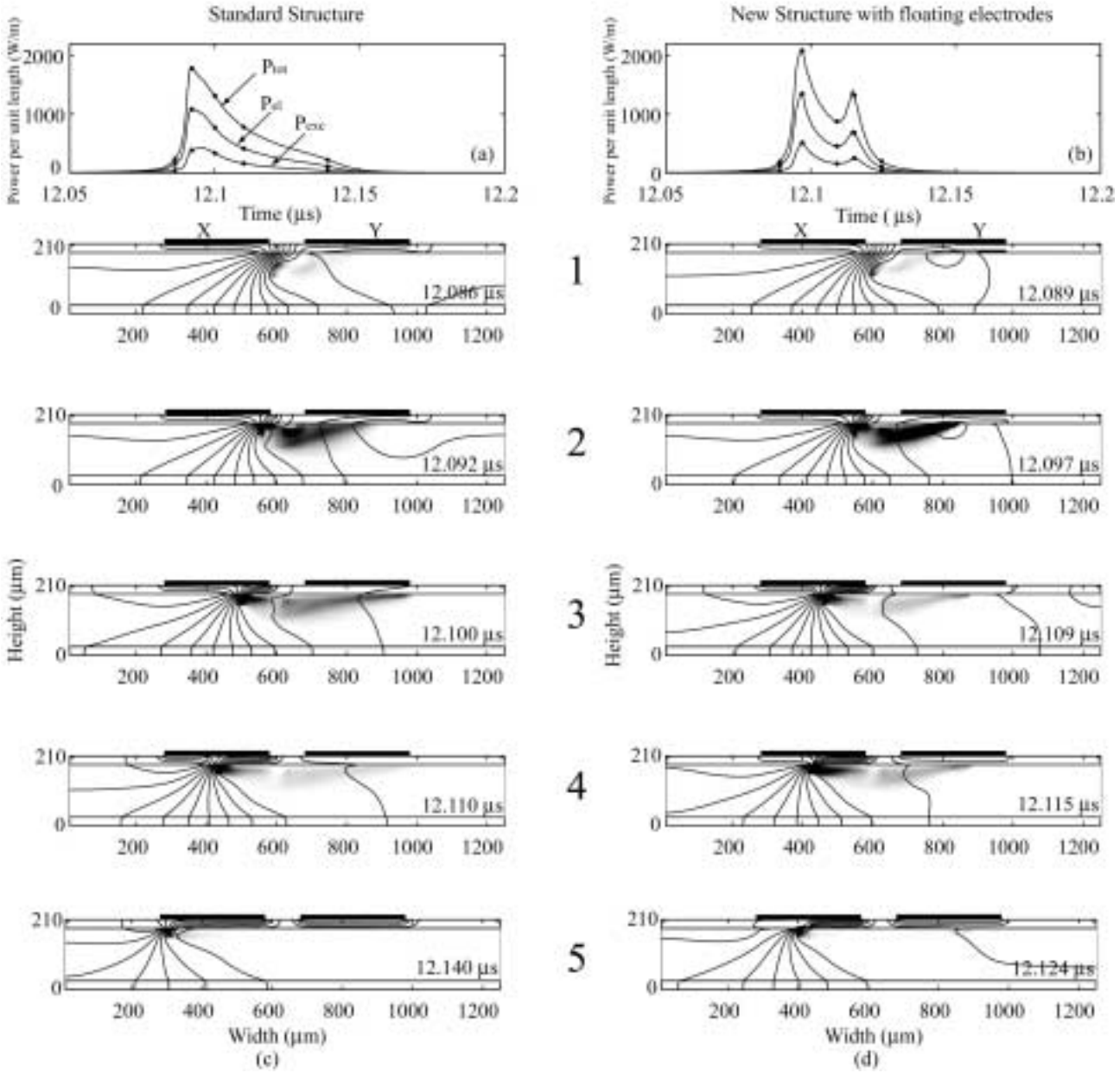

Figure 2. (a), (b) P_{tot}, P_{el}, P_{exc} for the standard and new structure respectively. (c), (d) Snapshots of power spent in Xe excitation and potential contours for the standard and new structure respectively.

3.2 Comparison with the Standard Case

We now compare the new cell structure geometry proposed in [3] with the standard cell geometry. In both cases, the coplanar electrode gap length g (Figure 1a) is set equal to 100 μm. In the standard case, the floating electrodes inserted in the upper dielectric layer are not included. In the new structure case, we choose the width w_f of the floating electrodes to be equal to 150 μm, and the vertical distance d_f between the sustain (X and Y) electrodes and the floating electrodes is set to 20 μm. In both cases, the amplitude of the initial pulse V_i is 290 V, and the amplitude of the sustain pulses V_s is 230 V.

In Figures 2a and 2b, we show the dissipated total power P_{tot}, dissipated electron power P_{el}, and power spent on Xe excitation P_{exc} in the PDP cell per unit length (the model is two-dimensional) for the standard and new structure cases respectively. Results are shown as a function of time, during the discharge caused by the 4th pulse applied to the Y electrode starting at t= 12 μs. We observe that the shape of the discharge power pulses are quite different, in agreement with the experimental results for the discharge current waveform reported in [3]. For the case of new cell structure, the voltage waveform has a double-pulse shape.

Figures 2c and 2d show snapshots of the power density spent on Xe excitation and potential contours for the standard and new structure cases respectively. The times corresponding to the snapshots are also shown in Figures 2a and 2b with dots for comparison. It should be noted that during the discharge caused by the 4th pulse, the Y electrode acts as the anode, while the X

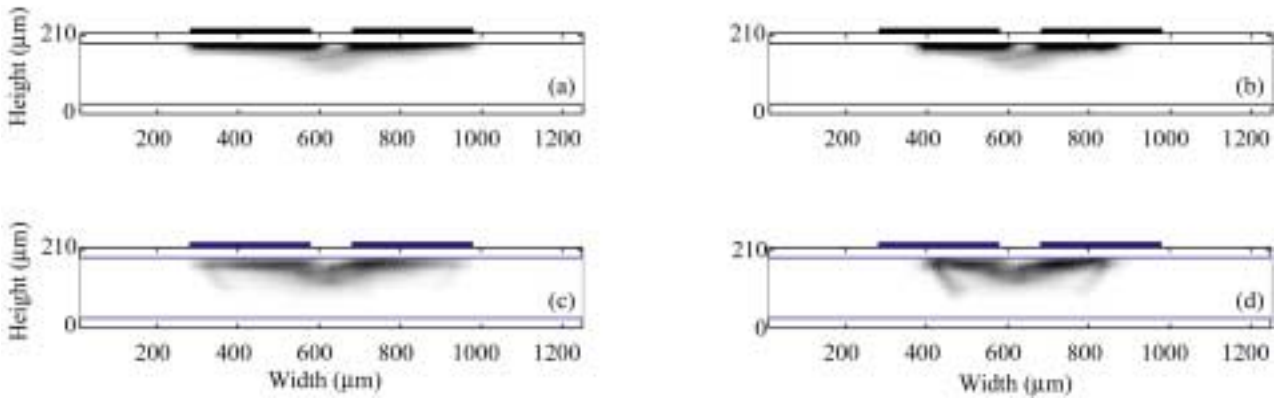

Figure 3. (a), (b) Dissipated energy density for the standard and new structure respectively. (c), (d) UV emission energy density for the standard and new structure respectively.

electrode acts as the cathode. In both cases, snapshot 1, corresponding to the initial stage of the discharge, shows that the spatial distribution of the Xe excitation is mostly confined at the interface between the expanding plasma and the ion sheath formed below the dielectric surface on the cathode side. In snapshot 2, corresponding to the maximum in power dissipation during the discharge, we observe that the Xe excitation power density is high both in the ion sheath–plasma interface and in the bulk of the plasma. The local maximum of excitation power in the bulk plasma region is close to the anode. Snapshot 3, corresponding to a later stage of the discharge, shows decrease of the excitation power density in both cases. The decrease is greater in the bulk of the plasma. The different behavior of the discharge for the two cases is illustrated in snapshots 4 and 5. In the standard case, the decrease of the excitation power density continues and the discharge power pulse smoothly decreases, as we observe in snapshot 4. The region of high Xe excitation is mostly confined at the ion sheath–expanding plasma interface. In the new structure case, a quite different behavior is observed. When the sheath–plasma interface reaches the cell area below the floating electrode, the discharge power increases. Snapshot 4 corresponds to the second maximum in power dissipation. We observe the spatial expansion of the high Xe excitation area towards the anode region with respect to the previous snapshot. Snapshot 5 corresponds to the final stage of the discharge in both cases. We observe that the region of high Xe excitation at the sheath–plasma boundary has shrank in both cases. In the standard case, the plasma expands until all the dielectric surface area below the cathode (X electrode) is covered with charge to screen the electric field of the 4th voltage pulse. In the new structure case, the plasma essentially expands only until it covers with charge the dielectric surface below the cathode before reaching the area below the floating electrode. In this area, the electric field of the voltage pulse is screened by charges on the floating electrode so that the corresponding dielectric surface does not have to be covered with charge. This also explains the shorter overall duration of the power pulse in the new structure case.

In Figures 3a and 3b, we show the dissipated energy density during the application of the 4 pulses (Figure 1b) for the standard and new structure cases respectively. In both cases, high dissipated energy density is observed in the regions directly below the dielectric layer covering the X and Y electrodes. This is expected since the local maxima of power density are always located in these regions. As we noted above, during each discharge there are two regions of high power dissipation. The first is in the ion sheath–plasma interface below the dielectric surface on the cathode side and the second is in the bulk of the plasma exhibiting a local maximum in the area below the dielectric surface on the anode side. We also observe that the high dissipated energy density region is more localized in the new structure case. This result can be explained by the partial screening of the voltage pulse electric field by the floating electrodes described above in detail (snapshot 5 in Figure 2d).

In Figures 3c and 3d, we show the total UV emission energy density integrated over all wavelengths considered (147 nm, 150 nm, and 173 nm) during the application of the 4 pulses (Figure 1b) for the standard and new structure cases respectively. We observe that UV emission is confined in the regions below the dielectric surface covering the X and Y electrodes. However, in both cases the region of high UV emission is wider when compared to the region of high dissipated energy density (shown in Figures 3a and 3b), extending towards the lower dielectric layer. This result is due to diffusion of some of the excited states of Xe which have long lifetimes. In addition, UV emission is more localized in the new structure case, since the region where power is spent by electrons in Xe excitation is more localized, as explained above (Figures 3a and 3b). The discharge current and UV emission confinement of the discharge by the new structure is expected to reduce cross talk between adjacent cells in agreement with the experimental findings reported in [3].

3.3 Parametric Studies

We now use the two-dimensional model to perform some parametric studies for the standard and new structure cases. We calculate the breakdown voltage for the geometry shown in Figure 1a. The breakdown voltage is directly related to the firing voltage V_f of the cell. We also calculate the UV efficiency, defined as the ratio of total UV energy spatially integrated over the gap to the total dissipated power.

In Figures 4a and 4b, we present results for the standard geometry, without inclusion of the floating electrodes shown in Figure 1a. In Figure 4a, we show the dependence of the breakdown voltage V_{br} on the coplanar electrode gap length g. V_{br} is an increasing function of g, as expected for the range of values of g studied. In Figure 4b, we show the dependence of the UV efficiency on the coplanar electrode gap length g. In all three cases (g= 80, 100, 140 μm), the amplitude of the initial pulse V_i (Figure 1b) is set to 25 V above the corresponding breakdown voltage V_{br}, and the amplitude of the sustain pulses V_s is set to 35

V below the corresponding breakdown voltage. The efficiency is an increasing function of g. However, increasing the gap length g is not a practical way of increasing the efficiency, since the operating voltages also increase.

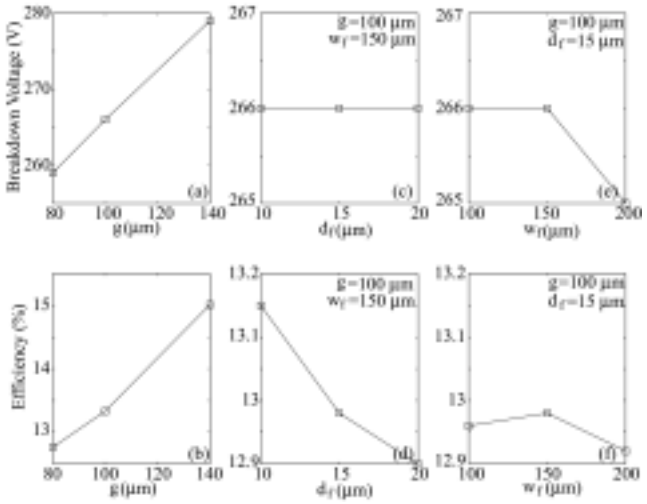

Figure 4. (a), (b) Breakdown voltage and UV efficiency as a function of the coplanar electrode length g for the standard structure. (c), (d) Breakdown voltage and UV efficiency as a function of d_f for the new structure. (e), (f) Breakdown voltage and UV efficiency as a function of w_f for the new structure.

In Figures 4c, 4d, 4e, and 4f we show results for the new geometry case (with floating electrodes). The coplanar electrode gap length g (Figure 1a) is set equal to 100 μm. In all cases, efficiency is measured by setting the amplitude of the initial pulse V_i (Figure 1b) to 25 V above the corresponding breakdown voltage V_{br}, and the amplitude of the sustain pulses V_s to 35 V below the corresponding breakdown voltage, as was also done in the standard geometry case.

In Figures 4c and 4d, we show the effect of the variation of the vertical distance d_f between the sustain (X and Y) electrodes and the floating electrodes on the breakdown voltage and the efficiency. We choose the floating electrodes' width w_f to be equal to 150 μm. We observe that the breakdown voltage exhibits essentially no variation with d_f. In addition, the breakdown voltage is almost equal to the corresponding one of the standard geometry. This result is in agreement with the experimental results reported in [3]. The UV efficiency slightly decreases with d_f; however, when compared with the UV efficiency of the standard geometry for the same electrode gap length g, it is found to be almost the same. Thus, the substantial increase of efficiency reported to be measured in [3] is not reproduced by the numerical simulation.

In Figures 4e and 4f, we show the effect of the variation of the floating electrodes' width w_f on the breakdown voltage and the efficiency. We choose the vertical distance d_f between the sustain (X and Y) electrodes and the floating electrodes to be equal to 15 μm. Again, we observe that the breakdown voltage exhibits essentially no variation with w_f, being almost equal to the corresponding one of the standard geometry. The UV efficiency shows no variation with w_f, being almost the same with the corresponding value for the standard geometry.

4. Summary

We use a two-dimensional model to study the effect of the insertion of a conducting material between the dielectric layer and the MgO film on the performance of a PDP cell. We find that the shape and the duration of the discharge power pulse are significantly different in comparison with the corresponding pulse of the standard cell geometry. This cell structure is found to result in a more confined discharge due to the partial screening of the voltage pulse electric field by the conducting material. The confinement of the discharge is expected to reduce cross talk between adjacent cells. In addition, the breakdown voltage of the new structure is essentially the same with the corresponding one of the standard geometry. These results are in good agreement with the experimental findings reported in [3]. The UV efficiency of the new structure is found to be the same as the one of the standard structure. The measured substantial increase of efficiency reported in [3] is not reproduced by the numerical simulation.

5. Acknowledgements

We greatly appreciate discussions with Prof. Victor Pasko of Pennsylvania State University. This work was supported by the Office of Technology Licensing of Stanford University under Grant No. 127P316.

6. References

[1] Punset, C., S. Cany, and J.-P. Boeuf, Addressing and sustaining in alternating current coplanar plasma display panels, J. Appl. Phys., 86, 124, 1999.

[2] Rauf, S., and M. J. Kushner, Dynamics of a coplanar-electrode plasma display panel cell. II. Cell optimization, J. Appl. Phys., 85, 3471, 1999.

[3] Kim J. S., C. H. Jeon, E. C. Lee, Y. J. Ahn, S. D. Kang, S. Y. Ahn, Y. K. Shin, J. H. Ryu, J. D. Schemerhorn, Application of a new panel structure for high luminous efficiency in AC-PDPs, SID Digest, 00, 102, 2000.

[4] Morgan W. L., and B. M. Penetrate, ELENDIF: A time-dependent Boltzmann solver for partially ionized plasmas, Comput. Phys. Commun., 58, 127, 1990.

[5] Ventzek P. L. G., R. J. Hoekstra, and M. J. Kushner, Two-dimensional modeling of high plasma density inductively coupled sources for materials processing, J. Vac. Sci. Technol. B, 12, 461, 1994.

[6] Hockney R. W., and J. W. Eastwood, Computer Simulation Using Particles. McGraw-Hill, New York, 1981, p. 215.